Published in final edited form as:
Biomaterials. 2013 September ; 34(28): 6957–6966. doi:10.1016/j.biomaterials.2013.05.063.

Long-Term Nitric Oxide Release and Elevated Temperature Stability with *S*-Nitroso-*N*-acetylpenicillamine (SNAP)-Doped Elast-eon E2As Polymer

Elizabeth J. Brisbois[a], **Hitesh Handa**[b], **Terry C. Major**[b], **Robert H. Bartlett**[b], and **Mark E. Meyerhoff**[a,*]

[a]Department of Chemistry, University of Michigan, Ann Arbor, MI USA

[b]Department of Surgery, University of Michigan, Ann Arbor, MI USA

Abstract

Nitric oxide (NO) is known to be a potent inhibitor of platelet activation and adhesion. Healthy endothelial cells that line the inner walls of all blood vessels exhibit a NO flux of 0.5~4×10^{-10} mol cm^{-2} min^{-1} that helps prevent thrombosis. Materials with a NO flux that is equivalent to this level are expected to exhibit similar anti-thrombotic properties. In this study, five biomedical grade polymers doped with *S*-nitroso-*N*-acetylpenicillamine (SNAP) were investigated for their potential to control the release of NO from the SNAP within the polymers, and further control the release of SNAP itself. SNAP in the Elast-eon E2As polymer creates an inexpensive, homogeneous coating that can locally deliver NO (via thermal and photochemical reactions) as well slowly release SNAP. Furthermore, SNAP is surprisingly stable in the E2As polymer, retaining 82% of the initial SNAP after 2 months storage at 37°C. The E2As polymer containing SNAP was coated on the walls of extracorporeal circuits (ECC) and exposed to 4 h blood flow in a rabbit model of extracorporeal circulation to examine the effects on platelet count, platelet function, clot area, and fibrinogen adsorption. After 4 h, platelet count was preserved at 100±7% of baseline for the SNAP/E2As coated loops, compared to 60±6% for E2As control circuits (n=4). The SNAP/E2As coating also reduced the thrombus area when compared to the control (2.3±0.6 and 3.4±1.1 pixels/cm^2, respectively). The results suggest that the new SNAP/E2As coating has potential to improve the thromboresistance of intravascular catheters, grafts, and other blood contacting medical devices, and exhibits excellent storage stability compared to previously reported NO release polymeric materials.

Keywords

biocompatibility; extracorporeal circulation; nitric oxide; platelets; *S*-nitrosothiols

*Corresponding Author: Dr. Mark E. Meyerhoff 930 N. University Ave. Ann Arbor, MI 48109 Telephone: (734) 763-5916 mmeyerho@umich.edu.

1. Introduction

Nitric oxide (NO) is an endogenous gas molecule that plays several key physiological roles, including prevention of platelet adhesion and activation, inhibiting bacterial adhesion and proliferation, enhancing vasodilation, promoting angiogenesis, and aiding in wound healing [1–10]. The effects of NO are highly dependent on the location and its concentration in the physiological system [11]. For example, endothelial cells that line the inner walls of healthy blood vessels produce an estimated NO surface flux of $0.5–4.0\times10^{-10}$ mol cm^{-2} min^{-1} [12]. The function of many blood-contacting devices, including vascular grafts, stents, intravascular sensors, intravascular catheters, and extracorporeal life support circuits, can be impaired due to platelet activation and thrombus formation [13, 14]. One approach to improve the hemocompatibility of such devices is the use of coating materials that mimic the endothelial cells with respect to NO release. Indeed, in recent years there has been considerable interest in developing NO-release and NO-generating materials that can be used to improve the biocompatibility of such devices [15–23].

Nitric oxide is highly reactive under physiological conditions and thus a wide range of NO donor molecules with functional groups that can store and release NO have been studied for potential biomedical applications. Such molecules include organic nitrates, metal-NO complexes, *N*-diazeniumdiolates, and *S*-nitrosothiols (RSNOs) [4, 24]. Physiological RSNOs, such as *S*-nitrosohemoglobin and *S*-nitrosoglutathione (GSNO), are considered an endogenous reservoir of NO *in vivo* [4, 25–27]. Other synthetic RSNOs, such as *S*-nitroso-*N*-acetyl-*L*-cysteine (SNAC) and *S*-nitroso-*N*-acetylpenicillamine (SNAP, Fig. 1A) have been shown to exhibit significant antimicrobial and antithrombotic effects [28–31]. It has also been demonstrated that RSNOs are both vasodilators and potent inhibitors of platelet aggregation [32, 33]. RSNOs undergo thermal decomposition releasing NO and producing a corresponding disulfide species (RSSR), as shown in Fig. 1B. The NO release from RSNOs can be catalyzed by metal ions (e.g., Cu^{+}) [34] and by light, through the irradiation at energies that correspond to the *S*-nitroso absorption bands at 340 and/or 590 nm [35–37]. It has been suggested that the more potent activity of RSNOs vs. NO as antiplatelet agents arises from the enhanced stability of RSNOs vs. NO, and generation of NO from RSNOs locally at the surface of platelets by membrane proteins that contain catalytic sites to convert RSNOs to NO [38].

Incorporation of RSNOs into polymers can extend the utility of these NO donors to be applicable as coatings in biomedical devices, providing localized NO release at the blood/device interface. Several NO-release polymers consisting of small-molecule RSNOs dispersed in various polymer matrices, including polyethylene glycol (PEG), poly(vinyl alcohol), poly(vinyl pyrrolidone), and Pluronic F127 hydrogel, have been reported [22, 23, 39–42]. These materials have potential applications for topical NO delivery on wounds via the diffusion of the hydrophilic RSNOs from the polymer to the tissue. In fact, daily application of a GSNO-containing hydrogel has been shown to accelerate the wound healing process [42]. However, the rapid leaching of the RSNOs from such polymers can significantly shorten the NO/RSNO release lifetime, lasting only several hours [22, 39, 40]. An alternate approach has been to synthesize RSNO-modified materials, where the RSNO functionality is covalently bound to the matrix. Fumed silica particles [18], dendrimers [43], polyurethanes [16], polyesters [15, 44–46], poly(dimethylsiloxane) (PDMS) [19], xerogels [47, 48], self-assembled monolayers [49], and poly(vinyl methyl ether-*co*-maleic anhydride) (PVMMA) [50] have all been modified with RSNO functionalities. Ricco et al. reported RSNO-modified xerogels that release NO for up to 14 d and exhibit reduced platelet and bacterial adhesion [47, 48]. However, such RSNO-modified xerogels suffer from synthesis complications leading to cracking and non-uniform films, low RSNO conversion efficiency (maximum of 40% for the tertiary RSNO-modified xerogels), and thermal instability at

room temperature that would limit their shelf-life. Many of the other RSNO modified materials reported to date exhibit both thermal and photoinitiated NO release, but these materials have not proven clinically useful due to their limited NO release lifetimes, low conversion to RSNO during synthesis, or lack of RSNO stability during storage This lack of stability of most NO release materials reported to date could pose a significant hurdle with regard commercializing medical devices that employ such materials, owing to the increased shipping costs to protect products from thermal degradation, etc. This could prevent the application of NO release materials in the biomedical market regardless of their potential benefits.

Another approach reported to achieve localized NO delivery at a polymer/blood interface is to use NO-generating coatings, in which immobilized catalysts (Cu(I/II) or organoselenium species) can generate NO from endogenous RSNOs [20, 51–53]. Recently, a NO generating coating containing Cu^0 nanoparticles was evaluated using a rabbit model for extracorporeal circulation (ECC) [20]. However, to achieve good efficacy in reducing thrombus formation, continuous infusion of SNAP was required to supplement the endogenous RSNO levels.

As an alternative to the continuous infusion of RSNO species, in this study we investigate several biomedical polymers that are capable of storing RSNO species. Such RSNO-doped coatings can release NO as well as potentially supplement the endogenous RSNO levels, if NO generating catalysts are also employed. Five biomedical polymers are examined for their potential to act as a storage reservoir for SNAP. These include: silicone rubber (poly(dimethylsiloxane)); Elast-eon E2As (a copolymer with a mixed soft segment of poly(dimethylsiloxane) and poly(hexamethylene oxide) with a methylene diphenyl isocyanate (MDI) hard segment); CarboSil (a thermoplastic urethane copolymer with a mixed soft segment of poly(dimethylsiloxane) and hydroxyl-terminated polycarbonate with a hard segment of an aromatic diisocyanate, MDI); Tecoflex SG80A (a poly(tetramethylene glycol) polyurethane capped with diisocyanatodicyclohexylmethane); and Tecophillic SP-60D-60 (an aliphatic, hydrophilic polyether-based polyurethane). Each of the SNAP-doped polymers are examined as films or coatings that can release NO thermally (at physiological temperature) and/or can serve as a reservoir to supplement endogenous RSNO levels (by SNAP diffusion into blood from the polymer). The SNAP-doped polymers are characterized for their *in vitro* NO/SNAP release, where the more hydrophobic polymers are expected to have slower SNAP/NO release under physiological conditions. The Elast-eon polymer has been reported to have excellent intrinsic biocompatibility and biostability properties, and exhibits low levels of blood protein adhesion [54, 55]. Therefore, the SNAP/E2As polymer is further tested for the stability of SNAP during a 2-month storage period, in order to ascertain any self-life concerns. The new SNAP/E2As polymer is also examined for potential biomedical applications via an ECC rabbit model of thrombogenicity to assess preservation of platelet count and function, and thrombus area after 4 h of ECC.

2. Materials and Methods

2.1. Materials

N-Acetyl-DL-penicillamine (NAP), sodium chloride, potassium chloride, sodium phosphate dibasic, potassium phosphate monobasic, ethylenediaminetetraacetic acid (EDTA), tetrahydrofuran (THF), sulfuric acid and *N,N*-dimethylacetamide (DMAc) were purchased from Sigma-Aldrich (St. Louis, MO). Methanol, hydrochloric acid and sulfuric acid were obtained from Fisher Scientific (Pittsburgh, PA). Tecophilic SP-60D-60 and Tecoflex SG-80A were products of Lubrizol Advanced Materials Inc. (Cleveland, OH). Dow Corning RTV 3140 Silicone Rubber (SR) was purchased from Ellsworth Adhesives (Germantown, WI). CarboSil 20 90A was from the Polymer Technology Group (Berkeley, CA). Elast-eon™ E2As was obtained from AorTech International, plc (Scoresby, Victoria, Australia).

Human plasma fibrinogen containing ≥ 90% clottable proteins was a product of Calbiochem (La Jolla, CA) and fluorescein-labeled goat IgG (polyclonal) against denatured human fibrinogen was purchased from MP Biomedicals, LLC (Solon, OH). Black, polypropylene 96-well microtiter plates used for fluorescence measurements were obtained from Nalge Nunc International (Rochester, NY). All aqueous solutions were prepared with 18.2 MΩ deionized water using a Milli-Q filter (Millipore Corp., Billerica, MA). Phosphate buffered saline (PBS), pH 7.4, containing 138 mM NaCl, 2.7 mM KCl, 10 mM sodium phosphate, 100μM EDTA was used for all *in vitro* experiments.

2.2. Synthesis of SNAP

SNAP was synthesized using a modified version of a previously reported method [56]. Briefly an equimolar ratio of NAP and sodium nitrite was added to a 1:1 mixture of water and methanol containing 2 M HCl and 2 M H_2SO_4. After 30 min of stirring, the reaction vessel was cooled in an ice bath to precipitate the green SNAP crystals. The crystals were collected by filtration, washed with water, and allowed to air dry. The reaction and crystals were protected from light at all times.

2.2. Preparation of SNAP-doped films

Polymer films containing 5 and 10 wt% SNAP were prepared by solvent evaporation. For the 10 wt% SNAP films, the casting solutions were prepared by dissolving 180 mg of the respective polymer in THF. The polyurethanes (SP-60D-60, SG-80A, CarboSil and Elast-eon E2As) were dissolved in 3 mL THF and SR was dissolved in 1 mL THF. SNAP (20 mg) was then added to the polymer solution and the mixture was stirred for 10 min. The 5 wt% SNAP films were prepared similarly with SNAP (10 mg) and polymer (190 mg). The film solution was cast in Teflon ring (d=2.5 cm) on a Teflon plate and dried overnight under ambient conditions. Small disks (d=0.7 cm) were cut from the parent films and were dip coated 2 times with a topcoat solution (200 mg polymer (no SNAP added) in 4 mL THF) and dried overnight under ambient conditions, followed by 48 h of drying under vacuum to remove any residual solvent. The weight of each small disk was recorded prior to top coating. All films and film solutions were protected from light. The thickness of the films before and after dip coating was measured using a Mitutoya digital micrometer. The final films had a SNAP-doped layer that was ~150 μm thick and a top coat layer that was ~50 μm thick.

2.3. Preparation of SNAP/E2As coated ECC loops

The ECC configuration employed in the *in vivo* rabbit study was previously described [20, 21]. Briefly, the ECC consisted of a 16-gauge and 14-gauge IV polyurethane angiocatheters (Kendall Monoject Tyco Healthcare Mansfield, MA), two 16 cm in length ¼ inch inner diameter (ID) Tygon™ tubing and an 8 cm length of 3/8 inch ID Tygon™ tubing that created a thrombogenicity chamber where thrombus could form more easily due to more turbulent blood flow.

Due to the short duration of the ECC experiments (4 h), the NO release ECC loops were coated with only 5 wt% SNAP in E2As. The SNAP/E2As solution was prepared by dissolving SNAP (125 mg) and E2As (2375 mg) in THF (15 mL). The E2As control solution consisted of E2As in THF (2500 mg in 15 mL). SNAP/E2As loops were first coated with 2 layers of the SNAP/E2As solution, followed by 1 coat of the E2As control solution. E2As control loops were coated with 2 coats of the E2As control solution. ECC loops were allowed to air dry for 1 h in the dark between each coat. The completely coated ECC was welded together using THF, starting at the left carotid artery side, with the 16-gauge angiocatheter, one 15 cm length ¼ inch ID tubing, the 8 cm length thrombogenicity chamber, the second 15 cm length ¼ inch ID tubing and finally the 14-gauge angiocatheter.

The angiocatheters were interfaced with tubing using two luer-lock PVC connectors. The assembled ECC loops were dried under vacuum while protected from light for at least 48 h. Prior to the ECC experiment, the loops were filled with saline solution for overnight soaking, and this solution was discarded immediately before the rabbit experiment.

2.4. *In vitro* characterization of SNAP-doped films

2.4.1. UV-Vis spectra—All UV-Vis spectra were recorded in the wavelength range of 200–700 nm using a UV-Vis spectrophotometer (Lambda 35, Perkin-Elmer, MA) at room temperature. The presence of the S-NO group of SNAP provides characteristic absorbance maxima at 340 and 590 nm, corresponding to the $\pi \rightarrow \pi^*$ and $n_N \rightarrow \pi^*$ electronic transitions [22, 37, 50].

2.4.2 Diffusion of SNAP from SNAP-doped Polymer Films Immersed in PBS—Top coated films were placed in individual vials soaked in 10 mM PBS, pH 7.4, containing 100 μM EDTA to minimize any trace metal ion catalyzed decomposition of SNAP. Films were incubated in the dark at room temperature (22°C) or 37°C. At various time points the UV-Vis spectra of a 1 mL aliquot of the PBS was taken for rapid determination of the SNAP concentration. The aliquots were protected from light and were immediately returned to the sample vials for the duration of the experiment. The films were placed in fresh PBS buffer daily. The molar absorption coefficient for SNAP in PBS at 340 nm was determined to be: ε_{SNAP}=1024 M^{-1} cm^{-1}. PBS buffer was used as the blank. The % SNAP remaining in the film was determined by the difference between the amount of SNAP that had leached into the PBS and the initial amount of SNAP in the film.

2.4.3 Cumulative NO release from SNAP/E2As Films—After the 10 wt% SNAP in E2As films were prepared, the UV-Vis spectra were recorded of individual films dissolved in DMAc to determine the initial concentration of SNAP within the films (nmol SNAP/mg film). Equivalent films were then placed in individual vials containing 3 mL PBS (pH 7.4) containing 100 μM EDTA. Films were incubated under various conditions: RT under ambient light, 37°C under ambient light, 37°C in dark, and 37°C under a 100W floodlight. These experiments were conducted in a basement lab without any windows, so the fluorescent lights in the laboratory are referred to as ambient light. Films were placed in fresh PBS daily. At various time points, the films were dissolved in DMAc for rapid determination of the SNAP present in the film. The amount of NO released was determined indirectly from the amount of SNAP decomposed at various time points. The cumulative NO released over time ($[NO]_t$) was calculated by the difference between the initial amount of SNAP in the film ($[SNAP]_0$) and the amount of SNAP at time t ($[SNAP]_t$): $[NO]_t = [SNAP]_0 - [SNAP]_t$ (where concentrations are in nmol/mg film). This calculation was based on the fact that the decay of the 340 nm absorption band of SNAP is directly associated with the homolytic cleavage of the S-NO bond and concomitant NO release. The molar absorption coefficient for SNAP in DMAc at 340 nm was determined to be: ε_{SNAP}=1025 M^{-1} cm^{-1}. DMAc was used as the blank.

2.4.4. NO Release Measurements—Nitric oxide released from the films was measured using a Sievers chemiluminescence Nitric Oxide Analyzer (NOA) 280 (Boulder, CO). Films were placed in the sample vessel immersed in PBS (pH 7.4) containing 100 μM EDTA. Nitric oxide was continuously purged from the buffer and swept from the headspace using an N_2 sweep gas and bubbler into the chemiluminescence detection chamber. Clear glass sample vessels were used for the ambient light and photoinitiated NO release experiments. A 100W halogen floodlight (GE model 17986) was used as a broad spectrum light source to initiate NO release and was placed ~60 cm from the sample cell for the photolysis

experiments. Films were incubated in the PBS under the same conditions as the NOA measurements (ambient light or 100W floodlight irradiation at 37°C).

2.4.5. SNAP/E2As Stability Study—SNAP/E2As films (consisting of 10 wt% SNAP) were placed under the following conditions in vials with desiccant: room temperature with ambient light, room temperature in dark, 37°C in dark, 50°C in dark, and in the freezer (−20°C) in dark. At various time points over a 2 month period, films were dissolved in DMAc and the UV-Vis spectra was recorded to determine the % SNAP remaining in the film, as compared to the initial 10 wt% SNAP.

2.4.6. In vitro Fibrinogen Adsorption Assay—The *in vitro* fibrinogen adsorption immunofluorescence assay was performed in a 96-well format. The SNAP/E2As and E2As control polymer solutions used to prepare the ECC circuits were also employed to coat microwells of the 96-well microtiter plates and were dried under the same conditions as the ECC loops. Briefly, human fibrinogen was diluted to 3 mg/mL with Dulbecco's phosphate-buffered saline (dPBS) without $CaCl_2$ and $MgCl_2$ (Gibco Invitrogen, Grand Island, NY), equivalent to the human plasma concentration, and then used for adsorption experiments [20]. One hundred μL of this solution were added to each well and the coated wells were incubated with this solution for 1.5 h at 37°C. This was followed by eight washing steps using wash buffer (100 μL) for each wash, which consisted of a 10-fold dilution of the AbD Serotec Block ACE buffer (Raleigh, NC) containing 0.05% Tween 20 (Calbiochem La Jolla, CA). To block nonspecific antibody binding, coated wells were incubated with 100 μL of blocking buffer (4-fold dilution of Serotec Block ACE buffer) for 30 min at 37°C. After rinsing 3 times with wash buffer (100 μL per well), a background fluorescence measurement of the plates was performed at 485 nm (excitation) and 528 nm (emission) on a Synergy 2 fluorescence microplate reader (Biotek Winooski, VT). To detect the adsorbed fibrinogen, fluorescein-labeled goat anti-human fibrinogen antibody was diluted (1:10) in a 10-fold dilution of the Serotec Block ACE buffer and 100 μL of this final solution was added to each well. The antibody was allowed to bind to the surface-adsorbed fibrinogen for 1.5 h at 37°C. Human fibrinogen adsorption to non-coated polypropylene was used as an internal control to normalize the fluorescence signals within different plates. All measurements were conducted in triplicate.

2.5. Rabbit ECC Thrombogenicity Experiments

All animal handling and surgical procedures employed were approved by the University Committee on the Use and Care of Animals in accordance with university and federal regulations. A total of 8 New Zealand white rabbits (Covance, Battle Creek, MI) were used in this study. All rabbits (2.5–3.5 kg) were initially anesthetized with intramuscular injections of 5 mg/kg xylazine injectable (AnaSed® Lloyd Laboratories Shenandoah, Iowa) and 30 mg/kg ketamine hydrochloride (Hospira, Inc. Lake Forest, IL). Maintenance anesthesia was administered via isoflurane gas inhalation at a rate of 1.5–3% via mechanical ventilation which was done via a tracheotomy and using an A.D.S. 2000 Ventilator (Engler Engineering Corp. Hialeah, FL). Peek inspiratory pressure was set to 15 cm of H_2O and the ventilator flow rate set to 8 L/min. In order to aid in maintenance of blood pressure stability, IV fluids of Lactated Ringer's were given at a rate of 10 mL/kg/h. For monitoring blood pressure and collecting blood samples, the rabbits' right carotid artery were cannulated using a 16-gauge IV angiocatheter (Jelco®, Johnson & Johnson, Cincinnati, OH). Blood pressure and derived heart rate were monitored with a Series 7000 Monitor (Marquette Electronics Milwaukee, WI). Body temperature was monitored with a rectal probe and maintained at 37°C using a water-jacketed heating blanket. Prior to placement of the arteriovenous (AV) custom-built extracorporeal circuit (ECC), the rabbit left carotid artery and right external jugular vein were isolated and baseline hemodynamics as well as arterial blood pH, PCO_2,

PO_2, total hemoglobin and methemoglobin were measured using an ABL 825 blood-gas analyzer and an OSM3 Hemoximeter (Radiometer Copenhagen, DK). In addition, baseline blood samples were collected for platelet and total white blood cell (WBC) counts which were measured on a Coulter Counter Z1 (Coulter Electronics Hialeah, FL). Plasma fibrinogen levels were determined using a Dade Behring BCS Coagulation Analyzer (Siemens Deerfield, IL), activated clotting times (ACT) were monitored using a Hemochron Blood Coagulation System Model 801 (International Technidyne Corp. Edison, NJ), and platelet function was assessed using a Chrono-Log optical aggregometer model 490 (Havertown, PA).

After baseline blood measurements, the AV custom-built ECC was placed into position by cannulating the left carotid artery for ECC inflow and the right external jugular vein for ECC outflow. The flow through the ECC was initiated by unclamping the arterial and venous sides of ECC and blood flow in circuit was monitored with an ultrasonic flow probe and flow meter (Transonic HT207 Ithaca, NY). Animals were not systemically anticoagulated during the experiments.

After 4 h on ECC, the circuits were clamped, removed from animal, rinsed with 60 mL of saline and drained. Any residual thrombus in the larger tubing of ECC (i.e., thrombogenicity chamber) was photographed and the degree of thrombus was quantitated using Image J imaging software from National Institutes of Health (Bethesda, MD). Prior to euthanasia, all animals were given a dose of 400 U/kg sodium heparin to prevent necrotic thrombosis. The animals were euthanized using a dose of Fatal Plus (130 mg/kg sodium pentobarbital) (Vortech Pharmaceuticals, Dearborn, MI). All animals underwent gross necropsy after being euthanized, including examination of the lungs, heart, liver and spleen for any signs of thromboembolic events.

2.6. Blood sampling

Rabbit whole blood samples were collected in non-anticoagulated 1 cc syringes for ACT, and in 3.2% sodium citrate vacutainers (Becton, Dickinson. Franklin Lakes, NJ) with 3 cc volumes for cell counts and aggregometry, and 1 cc syringes containing 40 U/mL of sodium heparin (APP Pharmaceuticals, LLC Schaumburg, IL) for blood-gas analysis. Following the initiation of ECC blood flow, blood samples were collected every hour for 4 h for these *in vitro* measurements. Samples were used within 2 h of collection to avoid any activation of platelets, monocytes or plasma fibrinogen.

2.7. Platelet Aggregometry

Rabbit platelet aggregation was assayed based on the Born's turbidimetric method using a Chrono-Log optical aggregometer. Briefly, citrated blood (1:10 blood to 3.2% sodium citrate solution) was collected (6 mL) and platelet-rich plasma (PRP) was obtained by centrifugation at 110 × g for 15 min. Platelet-poor plasma (PPP) was obtained by another centrifugation of the PRP-removed blood sample at 2730 × g for 15 min and was used as the blank for aggregation. PRP was incubated for 10 min at 37°C and then 25 μg/mL collagen (Chrono-PAR #385 Havertown, PA) was added. The percentage of aggregation was determined 3 min after the addition of collagen using Chrono-Log Aggrolink software.

Statistical Analysis: Data are expressed as mean ± SEM (standard error of the mean). Comparison between the various SNAP/E2As and E2As control polymer groups were analyzed by a comparison of means using student's *t*-test. Values of $p<0.05$ were considered statistically significant for all tests.

3. Results and Discussion

3.1 Preliminary *In Vitro* Characterization of Various SNAP-Doped Polymer Films

SNAP doped into all of the five biomedical polymers produced homogeneous and transparent films of green color, without any observable phase separation. The 10 wt% SNAP films stored approximately 0.42 μmol of SNAP per mg polymer film (or 6 μmol/cm^2). The diffusion of SNAP into PBS from the various polymer films containing 5 and 10 wt% SNAP was monitored using UV-Vis absorption. As shown in Fig. 2, which illustrates the calculated % SNAP remaining in the films, all of the SNAP diffuses out of the SG80A and SP-60D-60 polymer films during the first day of soaking in PBS at room temperature and at 37°C. The SP-60D-60 polymer is hydrophilic with a water uptake of ~60 wt%, while the SG80A is more hydrophobic, having a water uptake of ~ 6 wt% (see Table S1 in Supporting Information). All of the SNAP leaves the more hydrophilic SP-60D-60 polymer during the initial 2 h of soaking, while the more hydrophobic SG80A leaches all of the SNAP after 24 h. The diffusion of SNAP from the polymers occurs more rapidly at elevated temperatures (room temperature vs. 37°C) where the higher temperature allows for the polymer to more rapidly absorb water. Due to the rapid loss of the SNAP from the SP-60D-60 and SG80A polymers, a very large initial burst of NO is observed via chemiluminescence (with NOA) during the first day of soaking (Day 0) and the films exhibit no SNAP/NO release after one day (data not shown). Therefore, these two polymers only provide a quick burst of NO/SNAP and were found not to be suitable for longer-term release of NO/SNAP.

In contrast, the silicone rubber, CarboSil, and E2As polymers exhibit significantly lower amounts of SNAP diffusing into the soaking buffer after one day (see Fig. 2). For all three of these polymers, an initial burst of SNAP leaching is observed during the first day of soaking, corresponding to rapid water uptake by the polymer. This initial burst is ~10% of the total SNAP molecules incorporated into the films. Small amounts of SNAP continue to leach from these polymers during the subsequent days of soaking. Silicone rubber, CarboSil (a thermoplastic silicone-polycarbonate-urethane), and E2As (a siloxane-base polyurethane elastomer) all are hydrophobic polymers due to their high PDMS content [54, 57] and also have the lowest water uptake (see Table S1 in Supporting Information). SNAP is reported to be slightly hydrophobic [58]. Therefore, SNAP should have a preference for remaining in the more hydrophobic polymer phase. In addition, the hydrophobic property of these polymers also has a significant role in limiting the diffusion of SNAP into the buffer, due to the minimal water uptake of these polymers.

The thermal and photoinitiated NO release from the three SNAP-doped polymers was also studied by NOA measurements. Nitric oxide release can be turned on/off using the broad spectrum 100W floodlight for all 3 film types. As shown in Fig. 3A, there is little difference in the NO release from the films in the dark or under the ambient lab lights, since the ambient fluorescent laboratory lighting does not emit the wavelengths responsible for decomposing RSNOs (340 or 590 nm) [37]. Fluorescent lights emit discrete wavelengths of light, whereas the 100W halogen floodlight is a broad spectrum light source. For all three polymers, the total NO release detected by the NOA for films continuously irradiated with the 100W floodlight is ~100% of the SNAP doped into the films. The photoinitiated NO release from these three films was examined by continuously irradiating with a 100W floodlight at 37°C and monitoring the NO released with the NOA (Fig. 3B). The SNAP-doped E2As and CarboSil films exhibit a gradual decrease in the photo-induced NO flux over a 3 d period, while the SR-based films release NO for only 2 days under the same conditions. All three types of films incubated at 37°C under ambient light yielded an initial burst of NO on the first day of soaking, corresponding to release of SNAP into the solution, and on subsequent days, the NO flux is 1–2 × 10^{-10} mol cm^{-2} min^{-1}, still potentially useful

to inhibit platelet function and kill bacteria [11, 12]. The NO release is most promising from the film composed of 10 wt% SNAP in E2As under the 100W floodlight. Therefore, the wt % of SNAP in E2As was varied and examined in more detail (Fig. 3C). The NO release and SNAP leaching pattern is similar for a 5 wt% SNAP/E2As film, but the NO release takes place over a shorter time period. The biostability and biocompatibility of the Elast-eon polymers in combination with the NO release from SNAP makes this formulation most attractive for further *in vitro* studies and potential biomedical applications.

3.2. Long-Term NO Release of SNAP/E2As Formulation

In vitro studies were conducted with the SNAP/E2As films to examine the long-term NO release and SNAP leaching from these films. The NO release from the SNAP/E2As films over time was determined based on the amount of SNAP decomposed within the polymer phase (i.e., by measuring the SNAP remaining after dissolving the films at given time points). The initial concentration of SNAP in the 10 wt% films is 420 nmol SNAP/mg film. Fig. 4A shows the UV-Vis spectra of 1.0 mM SNAP solution, a 10 wt% SNAP in E2As film redissolved in *N,N*-dimethylacetamide (DMAc), and E2As dissolved in DMAc. Due to thermal and/or photochemical decomposition of SNAP, a decrease in the 340 nm absorbance band is observed as films are soaked in PBS and the cumulative NO release based on that absorbance decrease is shown in Fig. 4B. The films display an initial burst of NO during the first day of soaking (Fig. 2), which corresponds to the thermal decomposition as well as diffusion of SNAP out of the film. Films soaked at room temperature have the lowest flux of NO release. However, films incubated at 37°C in the dark or under ambient light exhibit a higher NO release than the films at room temperature. This is due to the increased thermal decomposition of SNAP. The films that are exposed to ambient light yield essentially the same NO release profiles as the films that are soaked in the dark. Nitric oxide release from the SNAP/E2As films that are continuously irradiated with the 100W floodlight at 37°C only release NO for 3 d due to their higher NO fluxes that rapidly deplete the SNAP reservoir. These films can provide NO release via both a thermal and photoinitiated decomposition of SNAP.

In order better understand the NO release mechanism of the SNAP/E2As coating, the SNAP diffusion into PBS was monitored over a 20 d period. As shown in Fig. 5A, the films containing 10 wt% SNAP at 37°C exhibit an initial burst of SNAP leaching on the first day. After this initial burst, small amounts of SNAP continue to slowly diffuse from the E2As until the SNAP reservoir is nearly depleted (with still measurable amounts of SNAP leaching on day 20). The total moles of SNAP that leach from the film accounts for ca. 27% of the total NO released (as detected by NOA measurements) during the 20 d period (see Fig. 5B), and thus the majority of the NO release can be attributed to the SNAP stored within the E2As film. Additionally, the effect of the number of polymer top coats on loss of SNAP was also evaluated. SNAP-doped E2As films without any top coat exhibit higher levels of SNAP diffusion into the buffer than films with at least 2 topcoats (see Fig. S1 in Supporting Information). The thickness of the top coat allows control of the diffusion rate of SNAP from the polymer reservoir.

Upon loss of NO as a result of photolysis or thermal effects, SNAP decomposes into NO and an organic radical that subsequently forms the disulfide dimer of *N*-acetylpenicillamine (NAP). NAP is a well-known heavy metal chelator that is used clinically in the treatment of methyl-mercury and copper poisoning [59–61]. Indeed, NAP has been used for almost half a century [62–65]. Its medical uses have been widely taught in Medical Pharmacology courses as part of heavy metal poisoning treatments [60, 61] and it has also been used to protect against free radical induced organ injuries [66]. Hence, some slight loss of NAP or the disulfide of NAP from the E2As polymer coatings would not likely create any toxicity issues if the proposed materials were ultimately employed for clinical applications.

3.3 Stability Study of the SNAP/E2As Films

The stability of SNAP doped in the E2As polymer during dry storage was also evaluated in order to ascertain the potential shelf-life of this material, as well a any thermal control requirements for storage and shipping. SNAP incorporated in E2As can potentially undergo thermal or photochemical decomposition during storage, thus limiting the available NO release capacity at the time of use. Therefore, SNAP/E2As films were stored dry in the dark with desiccant at room temperature and 37°C. These stability studies were conducted in a similar manner as the cumulative NO release experiments, where films were dissolved in DMAc to determine the amount of SNAP remaining in the polymer at various time points (as described in Section 2.4.5). Results indicate that SNAP is stable within the E2As polymer matrix after 2 months when stored at room temperature or at 37°C. The 10 wt% SNAP films stored in the freezer (−20°C) in the dark for 2 months maintain 96% of the initial SNAP species, compared to 89% for room temperature and 82% for films stored at 37°C (see Fig. 6). Additionally, SNAP films stored at 50°C retained 99% of the initial SNAP after 1 d storage, indicating that the SNAP within these films will likely withstand the slightly elevated temperatures used during ethylene oxide sterilization (1–6 h) that are required for clinical device applications. Tertiary RSNOs, such as SNAP, are known to have greater stability than primary RSNOs due to steric hindrance surrounding the sulfur atom [24, 58, 67]. The increased thermal stability of SNAP in combination with the stabilization effect of the E2As polymer allows provides excellent storage stability of the SNAP/E2As material.

Stability of RSNOs has been reported previously for viscous polymer matrices containing such NO donors, including poly(ethylene glycol), Pluronic F127 hydrogel, and poly(vinyl alcohol) and poly(vinyl pyrroloidone) [22, 23, 39, 40]. RSNOs decompose according to the following sequence of reactions:

$$\mathrm{RSNO} \rightarrow \mathrm{RS}^{\cdot} + \mathrm{NO}^{\cdot} \quad (1)$$

$$\mathrm{RS}^{\cdot} + \mathrm{RSNO} \rightarrow \mathrm{RSSR} + \mathrm{NO}^{\cdot} \quad (2)$$

$$\text{With the overall reaction: } 2\mathrm{RSNO} \rightarrow \mathrm{RSSR} + 2\mathrm{NO}^{\cdot} \quad (3)$$

The viscosity of the polymer matrix provides a cage effect on the bond cleavage and radical pair recombination [23]. In addition, a viscous polymer matrix also limits the diffusion of the radical species, favoring geminate recombination to reform RSNO. Thus, the E2As polymer not only limits the diffusion of SNAP into the PBS, but it also appears to provide an additional stabilization effect to reduce the rate of SNAP decomposition.

3.4. SNAP/E2As Coated ECC Loops and Effects on Rabbit Hemodynamics

In order to ascertain the potential benefits of the SNAP/E2As as a thromboresistant coating, a short-term ECC study was conducted to observe the effects of NO release from this new coating on platelets and thrombus area during 4 h blood flow. The active ECC loops coated with 5 wt% SNAP in E2As (Fig. 7) and control loops coated with E2As only were prepared. Five wt% SNAP was used in these tests due to the short duration of the ECC experiment. As described above, the SNAP/E2As coating has an initial burst of SNAP diffusing into solution during the first day of soaking. To reduce the effects of this burst during the short-term ECC experiments, all loops were first soaked overnight in saline and the soaking solution was discarded prior to the ECC experiments. Nitric oxide released from samples of the coated ECC loops were measured with the NOA for NO release before blood exposure (after overnight soaking in saline). The NO release of the SNAP/E2As coated loops

maintain an average flux of approximately 2×10^{-10} mol cm^{-2} min^{-1} for 4 h (at 37°C with ambient light). After 4 h of exposure to flowing blood, the ECC loops still exhibit a NO flux of at least 1.5×10^{-10} mol cm^{-2} min^{-1} for at an additional 1 h period (see Fig. S2 in Supporting Information).

The hemodynamic effects of the SNAP/E2As coated ECC circuits were also monitored over the 4 h of blood exposure in the rabbit ECC model. The mean arterial pressure (MAP) dropped significantly for both SNAP/E2As and control loops within the first hour, dropping to 35±2 and 46±2 mmHg, respectively. The MAP was maintained at these levels for the 4 h by continuous IV fluid maintenance. The ECC blood flow dropped and remained at 64±5 mL/min for SNAP/E2As ECC, but maintained at baseline levels over the 4 h (76±6 mL/min) for controls. The MAP drop and slower blood flow for the SNAP/E2As circuits is likely due to the vasodilatory effects of SNAP diffusing from the coating into the blood. The heart rate is maintained over the 4 h and no significant difference was noted between the SNAP/E2As and control ECC loops, averaging 205±2 beats/min. The activated clotting time increased over the 4 h period for both SNAP/E2As and control circuits, likely due to the increase in intravascular fluids (the hemodilution effect). Similar effects on MAP and flow rate were observed with SNAP infusion [20].

3.5 Effects of SNAP/E2As Coatings on Rabbit Platelet Function and Thrombus Formation

Platelet activation and function throughout the 4 h ECC was assessed by recording the platelet count and plasma fibrinogen levels (Fig. 8), which were both corrected for hemodilution due to the added IV fluids, as well as % platelet aggregation. The baseline platelet counts ($\times 10^8$ platelets/mL) were 3.5±0.6 and 4.8±0.5 for the SNAP/E2As and E2As control circuits, respectively. For the SNAP/E2As circuits, the platelet count initially rose slightly and was maintained at 100±7% of baseline levels at the end of 4 h on ECC. The platelet count for control circuits exhibited a time-dependent loss in platelets, dropping to 60±6% of baseline after 4 h. The percent of platelet functional aggregation was determined by *ex vivo* collagen stimulation of PRP and measured by optical turbidity. The platelets from blood taken from circulation through the SNAP/E2As and control circuits showed similar response to collagen-stimulated platelet aggregation during the 4 h blood exposure, both maintaining 56±12% (with baseline values at 68±6%).

Plasma fibrinogen levels were maintained at baseline levels for the control circuits (see Supporting Information, Fig. S3). For the SNAP/E2As circuits, the plasma fibrinogen levels during the first hour of ECC dropped to 83% of baseline levels and remained at that level for the 4 h ECC. This decrease in plasma fibrinogen levels can be attributed to fibrinogen binding to the surfaces, as shown by the *in vitro* fibrinogen assay (see Fig. S3 in Supporting Information). Surprisingly, even with the enhanced adsorption of fibrinogen on the SNAP/E2As coatings, these materials still exhibited significantly less platelet loss than controls, suggesting that the levels of NO produced overcome the enhanced fibrinogen adsorption that would normally enhance activation of platelets. To determine the differential formation of thrombus in the thrombogenicity chamber of the ECC circuit (i.e., the 3/8 inch ID Tygon™ tubing, 8 cm in length within the ECC loop), 2-dimensional (2D) image analysis was performed after 4 h of blood exposure. The thrombus area was analyzed by using Image J software and represents the 2D area of thrombus formation (pixels/cm^2) in each thrombogenicity chamber. The thrombus area was quantitated and data are shown in Fig. 9. The thrombus area is significantly reduced for the SNAP/E2As circuits when compared to controls, although the E2As controls also had relatively low thrombus area, likely resulting from the enhanced intrinsic biocompatibility of the E2As polymer [54, 55].

One of the effects of the new SNAP/E2As coating is the hypotension caused by the diffusion of SNAP into the blood stream, although the co-administration of intravenous fluids was

able to counteract this. The ECC loops used in this study had 1 top-coat layer; however additional top coat layers could be added (see Fig. S1 in Supporting Information) to limit SNAP leaching and further reduce the observed hypotensive effect. Use of a thin outer layer of a highly crosslinked polymer could also be employed to further retard the leaching of SNAP from the E2As polymer. Applications of SNAP have been reported to cause hypotension [68, 69], hyperglycemia and impaired insulin secretion [69], and decreased cell viability [70–72]. Endogenous thiols and superoxide dismutase will reduce many of these adverse effects. The parent thiol, *N*-acetyl-DL-penicillamine (NAP), however, has been used clinically to treat mercury poisoning [73] and cystinuria [59] with minimal side effects. Although the SNAP/E2As coatings studied here do exhibit a hypotension effect, the daily levels of SNAP delivered by the coating are well below the reported levels causing the other adverse side effects described above. Future coatings should employ the use of more lipophilic RSNOs or combine the SNAP/E2As coating with an immobilized catalyst on the inner surface of the ECC tubing to decompose the RSNO before they can enter the flowing blood, creating a fully localized delivery of the NO.

4. Conclusions

In this study it has been shown that the Elast-eon E2As polymer is an excellent matrix to act as reservoir for SNAP, and the resulting films can be used for the controlled release of NO and SNAP. SNAP slowly diffuses from the polymer film, and NO release from the film/coating can be initiated by light and/or thermal decomposition when blood flows through an ECC loop. Light (in the form of surgical lights, LEDs, fiber optics, etc.) could potentially be employed to administer higher doses of NO in a clinical setting. A stability study demonstrates that SNAP is quite stable within the E2As matrix, even during storage at 37°C for up to 2 months, demonstrating the enhanced shelf-life and potential for shipping devices made with this material without need for thermal control. Further, our finding that SNAP in the E2As also survives 50°C for at least one day, indicates that ethylene oxide sterilization of medical devices that utilize the SNAP/E2As coating should be possible. While the E2As polymer has excellent innate biocompatible properties on its own, incorporating SNAP into the E2As polymer matrix provides controlled delivery of NO/SNAP to further improve polymer hemocompatibility. The SNAP/E2As coated ECC loops significantly preserved platelet count and function during 4 h of ECC blood flow, while also reducing the clot area when compared to corresponding E2As coated control loops. Incorporating SNAP within Elast-eon E2As polymer films/coatings provides a simple way to locally deliver NO/SNAP, and has potential for improving the hemocompatibility of a wide variety of blood-contacting medical devices, without risk of eluting any toxic precursor, given the use of NAP already as an approved therapeutic agent.

Supplementary Material

Refer to Web version on PubMed Central for supplementary material.

Acknowledgments

This work was supported by grants from the National Institutes of Health (EB-004527 and K25HL111213). The authors wish to thank AorTech International for the gift of Elast-eon E2As polymer.

References

[1]. Fang FC. Mechanisms of nitric oxide-related antimicrobial activity. J Clin Invest. 1997; 99:2818–25. [PubMed: 9185502]

[2]. Luo, J-d; Chen, AF. Nitric oxide: a newly discovered function on wound healing. Acta Pharmacol Sin. 2005; 26:259–64. [PubMed: 15715920]

[3]. Wallis JP. Nitric oxide and blood: a review. Transfus Med. 2005; 15:1–11. [PubMed: 15713123]

[4]. Williams DLH. A chemist's view of the nitric oxide story. Org Biomol Chem. 2003; 1:441–9. [PubMed: 12926240]

[5]. Baek SH, Hrabie JA, Keefer LK, Hou DM, Fineberg N, Rhoades R, et al. Augmentation of intrapericardial nitric oxide level by a prolonged-release nitric oxide donor reduces luminal narrowing after porcine coronary angioplasty. Circulation. 2002; 105:2779–84. [PubMed: 12057994]

[6]. Chaux A, Ruan XM, Fishbein MC, Ouyang Y, Kaul S, Pass JA, et al. Perivascular delivery of a nitric oxide donor inhibits neointimal hyperplasia in vein grafts implanted in the arterial circulation. J Thorac Cardiovasc Surg. 1998; 115:604–14. [PubMed: 9535448]

[7]. Gifford R, Batchelor MM, Lee Y, Gokulrangan G, Meyerhoff ME, Wilson GS. Mediation of in vivo glucose sensor inflammatory response via nitric oxide release. J Biomed Mater Res Part A. 2005; 75A:755–66.

[8]. Mellion BT, Ignarro LJ, Ohlstein EH, Pontecorvo EG, Hyman AL, Kadowitz PJ. Evidence for the inhibitory role of guanosine 3',5'-monophosphate in ADP-induced human platelet aggregation in the presence of nitric oxide and related vasodilators. Blood. 1981; 57:946–55. [PubMed: 6111365]

[9]. Nablo BJ, Rothrock AR, Schoenfisch MH. Nitric oxide-releasing sol-gels as antibacterial coatings for orthopedic implants. Biomaterials. 2005; 26:917–24. [PubMed: 15353203]

[10]. Radomski MW, Palmer RMJ, Moncada S. Comparative pharmacology of endothelium-derived relaxing factor, nitric oxide and prostacylin in platelets. Br J Pharmacol. 1987; 92:181–7. [PubMed: 3311265]

[11]. Davis KL, Martin E, Turko IV, Murad F. Novel effects of nitric oxide. Annu Rev Pharmacol Toxicol. 2001; 41:203–36. [PubMed: 11264456]

[12]. Vaughn MW. Estimation of nitric oxide production and reactionrates in tissue by use of a mathematical model. Am J Physiol Heart Circ Physiol. 1998; 274:H2163.

[13]. Ratner BD. The catastrophe revisited: blood compatibility in the 21st century. Biomaterials. 2007; 28:5144–7. [PubMed: 17689608]

[14]. Ratner BD, Bryant SJ. Biomaterials: where we have been and where we are going. Annu Rev of Biomed Eng. 2004; 6:41–75. [PubMed: 15255762]

[15]. Coneski PN, Rao KS, Schoenfisch MH. Degradable nitric oxide-releasing biomaterials via post-polymerization functionalization of cross-linked polyesters. Biomacromolecules. 2010; 11:3208–15.

[16]. Coneski PN, Schoenfisch MH. Synthesis of nitric oxide-releasing polyurethanes with S-nitrosothiol-containing hard and soft segments. Polym Chem. 2011; 2:906–13. [PubMed: 23418409]

[17]. Damodaran VB, Reynolds MM. Biodegradable S-nitrosothiol tethered multiblock polymer for nitric oxide delivery. J Mater Chem. 2011; 21:5870–2.

[18]. Frost MC, Meyerhoff ME. Synthesis, characterization, and controlled nitric oxide release from S-nitrosothiol-derivatized fumed silica polymer filler particles. J Biomed Mater Res Part A. 2005; 72A:409–19.

[19]. Gierke GE, Nielsen M, Frost MC. S-nitroso-N-acetyl-D-penicillamine covalently linked to polydimethylsiloxane (SNAP–PDMS) for use as a controlled photoinitiated nitric oxide release polymer. Sci Technol Adv Mat. 2011; 12:055007.

[20]. Major TC, Brant DO, Burney CP, Amoako KA, Annich GM, Meyerhoff ME, et al. The hemocompatibility of a nitric oxide generating polymer that catalyzes S-nitrosothiol decomposition in an extracorporeal circulation model. Biomaterials. 2011; 32:5957–69. [PubMed: 21696821]

[21]. Major TC, Brant DO, Reynolds MM, Bartlett RH, Meyerhoff ME, Handa H, et al. The attenuation of platelet and monocyte activation in a rabbit model of extracorporeal circulation by a nitric oxide releasing polymer. Biomaterials. 2010; 31:2736–45. [PubMed: 20042236]

[22]. Shishido, SlM; Seabra, AB.; Loh, W.; Ganzarolli de Oliveira, M. Thermal and photochemical nitric oxide release from S-nitrosothiols incorporated in Pluronic F127 gel: potential uses for local and controlled nitric oxide release. Biomaterials. 2003; 24:3543–53. [PubMed: 12809783]

[23]. Shishido SM, de Oliveira MG. Polyethylene glycol matrix reduces the rates of photochemical and thermal release of nitric oxide from S-nitroso-N-acetylcysteine. Photochem Photobiol. 2000; 71:273–80. [PubMed: 10732444]

[24]. Wang PG, Xian M, Tang XP, Wu XJ, Wen Z, Cai TW, et al. Nitric oxide donors: chemical activities and biological applications. Chem Rev. 2002; 102:1091–134. [PubMed: 11942788]

[25]. Al-Sa'doni H, Ferro A. S-nitrosothiols: a class of nitric oxide-donor drugs. Clin Sci (Lond). 2000; 98:507–20. [PubMed: 10781381]

[26]. Hogg N. Biological chemistry and clinical potential of S-nitrosothiols. Free Radic Biol Med. 2000; 28:1478–86. [PubMed: 10927172]

[27]. Hogg N, Singh RJ, Kalyanaraman B. The role of glutathione in the transport and catabolism of nitric oxide. FEBS Letters. 1996; 382:223–8. [PubMed: 8605974]

[28]. Langford EJ, Brown AS, Wainwright RJ, Debelder AJ, Thomas MR, Smith REA, et al. Inhibition of platelet activity by S-nitrosoglutathione during coronary angioplasty. Lancet. 1994; 344:1458–60. [PubMed: 7526102]

[29]. Radomski MW, Rees DD, Dutra A, Moncada S. S-nitroso-glutathione inhibits platelet activation in vitro and in vivo. Br J Pharmacol. 1992; 107:745–9. [PubMed: 1335336]

[30]. Salas E, Moro MA, Askew S, Hodson HF, Butler AR, Radomski MW, et al. Comparative pharmacology of analogues of S-nitroso-*N*-acetyl-DL-penicillamine on human platelets. Br J Pharmacol. 1994; 112:1071–6. [PubMed: 7524991]

[31]. de Souza GFP, Yokoyama-Yasunaka JKU, Seabra AB, Miguel DC, de Oliveira MG, Uliana SRB. Leishmanicidal activity of primary S-nitrosothiols against Leishmania major and Leishmania amazonensis: implications for the treatment of cutaneous leishmaniasis. Nitric Oxide-Biol Chem. 2006; 15:209–16.

[32]. Albert J, Daleskog M, Wallen NH. A comparison of the antiplatelet effect of S-nitrosoglutathione in whole blood and platelet-rich plasma. Thromb Res. 2001; 102:161–5. [PubMed: 11323027]

[33]. Ricardo KFS, Shishido SM, de Oliveira MG, Krieger MH. Characterization of the hypotensive effect of S-nitroso-N-acetylcysteine in normotensive and hypertensive conscious rats. Nitric Oxide-Biol Chem. 2002; 7:57–66.

[34]. Dicks AP, Swift HR, Williams DLH, Butler AR, AlSadoni HH, Cox BG. Identification of Cu+ as the effective reagent in nitric oxide formation from S-nitrosothiols (RSNO). J Chem Soc, Perkin Trans 2. 1996:481–7.

[35]. Sexton DJ, Muruganandam A, McKenney DJ, Mutus B. Visible light photochemical release of nitric oxide from *S*-nitrosoglutathione: potential photochemotherapeutic applications. Photochem Photobiol. 1994; 59:463–7. [PubMed: 8022889]

[36]. Wood PD, Mutus B, Redmond RW. The mechanism of photochemical release of nitric oxide from S-nitrosoglutathione. Photochem Photobiol. 1996; 64:518–24.

[37]. Frost MC, Meyerhoff ME. Controlled photoinitiated release of nitric oxide from polymer films containing S-nitroso-N-acetyl-DL-penicillamine derivatized fumed silica filler. J Am Chem Soc. 2004; 126:1348–9. [PubMed: 14759186]

[38]. Gordge MP, Hothersall JS, Neild GH, Dutra AAN. Role of a copper (I)-dependent enzyme in the anti-platelet action of S-nitrosoglutathione. Br J Pharmacol. 1996; 119:533–8. [PubMed: 8894174]

[39]. Seabra AB, de Souza GFP, da Rocha LL, Eberlin MN, de Oliveira MG. S-nitrosoglutathione incorporated in poly(ethylene glycol) matrix: potential use for topical nitric oxide delivery. Nitric Oxide-Biol Chem. 2004; 11:263–72.

[40]. Seabra AB, de Oliveira MG. Poly(vinyl alcohol) and poly(vinyl pyrrolidone) blended films for local nitric oxide release. Biomaterials. 2004; 25:3773–82. [PubMed: 15020153]

[41]. Seabra AB, Fitzpatrick A, Paul J, De Oliveira MG, Weller R. Topically applied S-nitrosothiol-containing hydrogels as experimental and pharmacological nitric oxide donors in human skin. Br J Dermatol. 2004; 151:977–83. [PubMed: 15541075]

[42]. Amadeu TP, Seabra AB, De Oliveira MG, Costa AMA. S-nitrosoglutathione-containing hydrogel accelerates rat cutaneous wound repair. J Eur Acad Dermatol Venereol. 2007; 21:629–37. [PubMed: 17447976]

[43]. Stasko NA, Fischer TH, Schoenfisch MH. S-nitrosothiol-modified dendrimers as nitric oxide delivery vehicles. Biomacromolecules. 2008; 9:834–41. [PubMed: 18247567]

[44]. Seabra AB, da Silva R, de Oliveira MG. Polynitrosated polyesters: preparation, characterization, and potential use for topical nitric oxide release. Biomacromolecules. 2005; 6:2512–20. [PubMed: 16153087]

[45]. Seabra AB, da Silva R, de Souza GFP, de Oliveira MG. Antithrombogenic polynitrosated polyester/poly(methyl methacrylate) blend for the coating of blood-contacting surfaces. Artif Organs. 2008; 32:262–7. [PubMed: 18370938]

[46]. Seabra AB, Martins D, Simoes M, da Silva R, Brocchi M, de Oliveira MG. Antibacterial nitric oxide-releasing polyester for the coating of blood-contacting artificial materials. Artif Organs. 2010; 34:E204–E14. [PubMed: 20497163]

[47]. Riccio DA, Coneski PN, Nichols SP, Broadnax AD, Schoenfisch MH. Photoinitiated nitric oxide-releasing tertiary S-nitrosothiol-modified xerogels. ACS Appl Mater Interfaces. 2012; 4:796–804. [PubMed: 22256898]

[48]. Riccio DA, Dobmeier KP, Hetrick EM, Privett BJ, Paul HS, Schoenfisch MH. Nitric oxide-releasing S-nitrosothiol-modified xerogels. Biomaterials. 2009; 30:4494–502. [PubMed: 19501904]

[49]. Etchenique R, Furman M, Olabe JA. Photodelivery of nitric oxide from a nitrosothiol-derivatized surface. J Am Chem Soc. 2000; 122:3967–8.

[50]. Li Y, Lee PI. Controlled nitric oxide delivery platform based on S-nitrosothiol conjugated interpolymer complexes for diabetic wound healing. Mol Pharm. 2009; 7:254–66. [PubMed: 20030413]

[51]. Puiu SC, Zhou Z, White CC, Neubauer LJ, Zhang Z, Lange LE, et al. Metal ion-mediated nitric oxide generation from polyurethanes via covalently linked copper(II)-cyclen moieties. J Biomed Mater Res B Appl Biomater. 2009; 91B:203–12. [PubMed: 19441117]

[52]. Yang J, Welby JL, Meyerhoff ME. Generic nitric oxide (NO) generating surface by immobilizing organoselenium species via layer-by-layer assembly. Langmuir. 2008; 24:10265–72. [PubMed: 18710268]

[53]. Oh BK, Meyerhoff ME. Spontaneous Catalytic Generation of Nitric Oxide from S-Nitrosothiols at the Surface of Polymer Films Doped with Lipophilic Copper(II) Complex. J Am Chem Soc. 2003; 125:9552–3. [PubMed: 12903997]

[54]. Cozzens D, Luk A, Ojha U, Ruths M, Faust R. Surface characterization and protein interactions of segmented polyisobutylene-based thermoplastic polyurethanes. Langmuir. 2011; 27:14160–8. [PubMed: 22023013]

[55]. Simmons A, Padsalgikar AD, Ferris LM, Poole-Warren LA. Biostability and biological performance of a PDMS-based polyurethane for controlled drug release. Biomaterials. 2008; 29:2987–95. [PubMed: 18436300]

[56]. Chipinda I, Simoyi RH. Formation and stability of a nitric oxide donor: S-nitroso-N-acetylpenicillamine. J Phys Chem B. 2006; 110:5052–61. [PubMed: 16526748]

[57]. Gunatillake PA, Martin DJ, Meijs GF, McCarthy SJ, Adhikari R. Designing biostable polyurethane elastomers for biomedical implants. Aust J Chem. 2003; 56:545–57.

[58]. Megson IL, Morton S, Greig IR, Mazzei FA, Field RA, Butler AR, et al. N-substituted analogues of S-nitroso-N-acetyl-D,L-penicillamine: chemical stability and prolonged nitric oxide mediated vasodilatation in isolated rat femoral arteries. Br J Pharmacol. 1999; 126:639–48. [PubMed: 10188974]

[59]. Stephens A, Watts R. The treatment of cystinuria with N-acetyl-D-penicillamine, a comparison with the results of D-penicillamine treatment. Q J Med. 1971; 40:355–70. [PubMed: 5564534]

[60]. Tiruppathi, C. Heavy metal toxicity: drug disposition and pharmacokinetics class. 2006. http://wwwuicedu/classes/pcol/pcol331/dentalpharmhandouts2006/lecture41pdf

[61]. Clarckson, C. Penicillamine_NAP. 2012. http://tmedwebtulaneedu/pharmwiki/dokuphp/penicillamine_nap

[62]. Gledhill R, Hopkins A. Chronic inorganic mercury poisoning treated with N-acetyl-D-penicillamine. Br J Ind Med. 1972; 29:225–8. [PubMed: 5022002]

[63]. Kark R, Poskanzer DC, Bullock JD, Boylen G. Mercury poisoning and its treatment with N-acetyl-D,L-penicillamine. N Engl J Med. 1971; 285:10. [PubMed: 5089366]

[64]. Parameshvara V. Mercury poisoning and its treatment with N-acetyl-D, L-penicillamine. Br J Ind Med. 1967; 24:73–6. [PubMed: 6017143]

[65]. Markowitz L, Schaumburg HH. Successful treatment of inorganic mercury neurotoxicity with N-acetyl-penicillamine despite an adverse reaction. Neurology. 1980; 30:1000. [PubMed: 7191527]

[66]. Srivastava P, Arif AJ, Singh C, Pandey VC. N-acetyl-penicillamine: a protector of *Plasmodium berghei* induced stress organ injury in mice. Pharmacol Res. 1997; 36:305–7. [PubMed: 9425620]

[67]. Lin CE, Richardson SK, Wang WH, Wang TS, Garvey DS. Preparation of functionalized tertiary thiols and nitrosothiols. Tetrahedron. 2006; 62:8410–8.

[68]. Rassaf T, Kleinbongard P, Preik M, Dejam A, Gharini P, Lauer T, et al. Plasma nitrosothiols contribute to the systemic vasodilator effects of intravenously applied NO - experimental and clinical study on the fate of NO in human blood. Circ Res. 2002; 91:470–7. [PubMed: 12242264]

[69]. McGrowder D, Ragoobirsingh D, Dasgupta T. Effects of S-nitroso-N-acetyl-penicillamine administration on glucose tolerance and plasma levels of insulin and glucagon in the dog. Nitric Oxide-Biol Chem. 2001; 5:402–12.

[70]. Fatokun AA, Stone TW, Smith RA. Prolonged exposures of cerebellar granule neurons to S-nitroso-N-acetylpenicillamine (SNAP) induce neuronal damage independently of peroxynitrite. Brain Res. 2008; 1230:265–72. [PubMed: 18644353]

[71]. Khalilmanesh F, Price RG. Effect of D-penicillamine on glomerular basement membrane, urinary *N*-acetyl-beta--D-glucosaminidase and protein excretion in rats. Toxicology. 1983; 26:325–34. [PubMed: 6857704]

[72]. Zamora R, Matthys KE, Herman AG. The protective role of thiols against nitric oxide-mediated cytotoxicity in murine macrophage J774 cells. Eur J Pharmacol. 1997; 321:87–96. [PubMed: 9083790]

[73]. Kark RAP, Poskanzer DC, Bullock JD, Boylen G. Mercury poisoning and its treatment with N-acetyl-D,L-penicillamine. N Engl J Med. 1971; 285:10–6. [PubMed: 5089366]

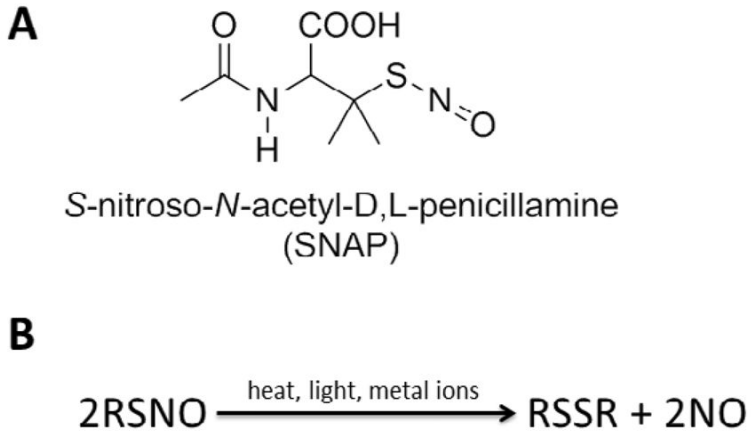

Fig. 1.

Structure of (A) *S*-nitroso-*N*-acetylpenicillamine (SNAP) and (B) scheme of *S*-nitrosothiol (RSNO) decomposition, which can be catalyzed by metal ions (e.g. Cu^{+}), light, and heat, yielding the disulfide (RSSR) product and nitric oxide (NO).

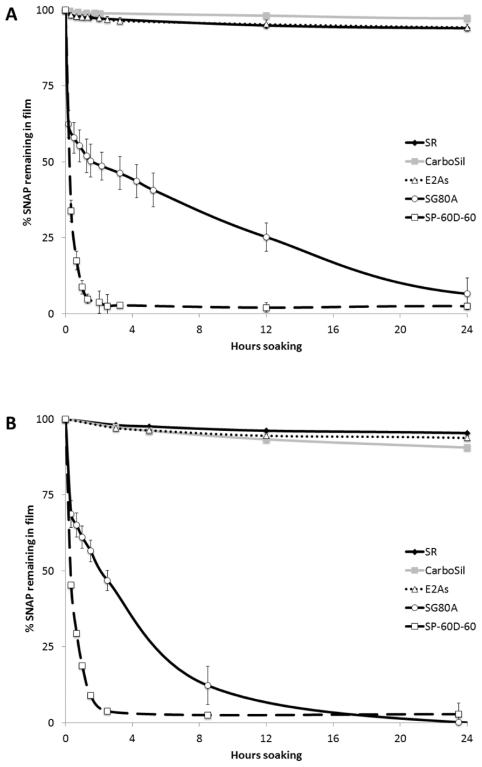

Fig. 2.

Percent of SNAP remaining in films (initially prepared with 10 wt% SNAP) after various durations of soaking in 4 mL PBS in the dark at room temperature, 22°C (A), or 37°C (B). Data is based on the difference between the amount of SNAP that leached from various polymers into the PBS, as monitored at 340 nm, and the initial amount of SNAP doped in the film. Data is the mean ± SEM (n=3).

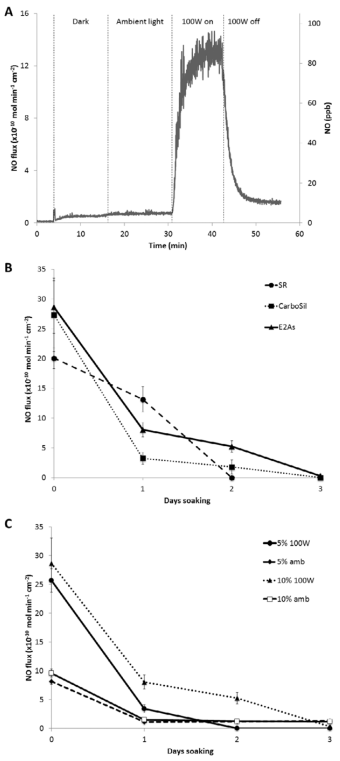

Fig. 3.

(A) NO release behavior of 10 wt% SNAP/E2As film at 37°C in the dark, ambient light, and 100W floodlight. (B) NO release from 10 wt% SNAP in silicone rubber (SR), CarboSil, and Elast-eon E2As films at 37°C and continuously irradiated with the 100W floodlight. (C) NO release from 5 and 10 wt% SNAP in Elast-eon E2As films at 37°C continuously under ambient light (amb) or the 100W floodlight. Data is the mean ± SEM (n=3).

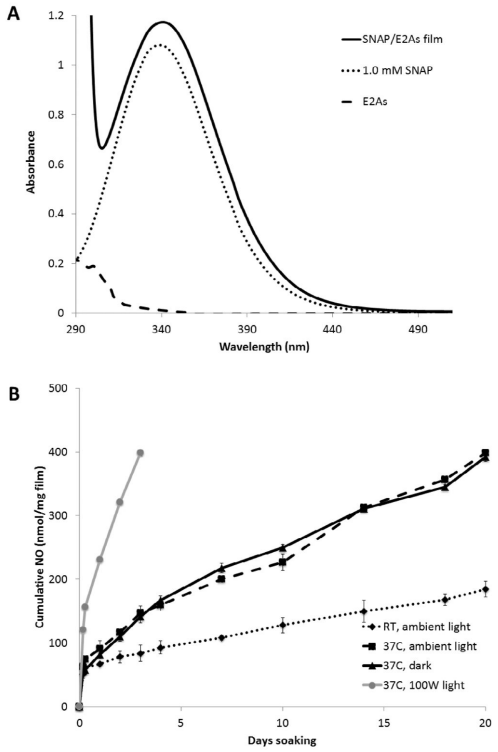

Fig. 4.

(A) UV-vis spectra of a 10 wt% SNAP/E2As film, 1.0 mM SNAP, and E2As dissolved in *N,N*-dimethylacetamide (DMAc). (B) Cumulative NO release from 10 wt% SNAP/E2As films incubated in PBS under various conditions: room temperature (22°C) with ambient light, 37°C in the dark, 37°C under ambient light, and 37°C under the 100W floodlight. Data is the mean ± SEM (n=3).

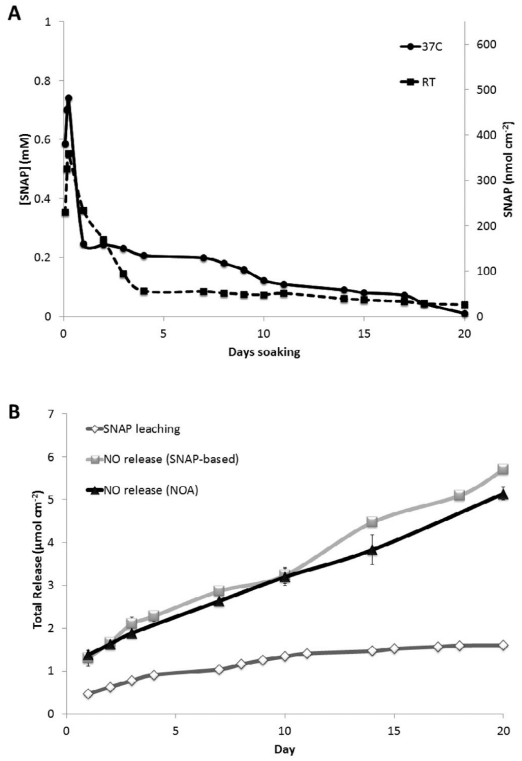

Fig. 5.

(A) Diffusion of SNAP from 10 wt% SNAP-doped E2As films soaking in 1 mL PBS in the dark, as monitored at 340 nm, at room temperature (RT, 22°C) or 37°C. (B) Comparison of the cumulative SNAP leaching and cumulative NO release (based on NOA-based or SNAP-based NO release data) from the 10 wt% SNAP-doped E2As films soaking in PBS at 37°C in the dark. Nitric oxide release from SNAP-doped E2As films can occur from thermal and/or photochemical decomposition of SNAP within the polymer phase, or from SNAP that leached into the aqueous phase. For the SNAP-doped E2As films, approximately 27% of the total NO release is attributed to the SNAP leaching.

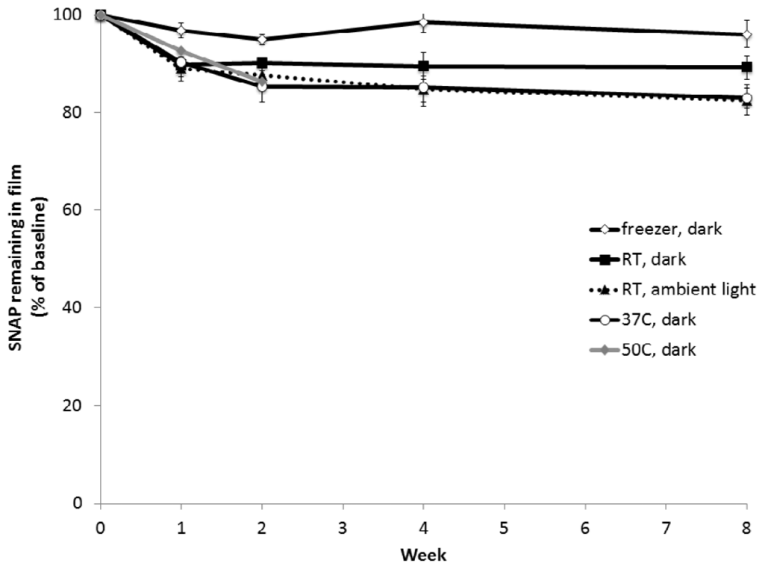

Fig. 6.

Stability of 10 wt% SNAP in E2As films stored dry with desiccant under various temperature and light conditions. Films were dissolved in DMAc to rapidly determine the amount of SNAP remaining at various times (compared to the initial level) as monitored at 340 nm by UV-vis. Data is the mean ± SEM (n=3).

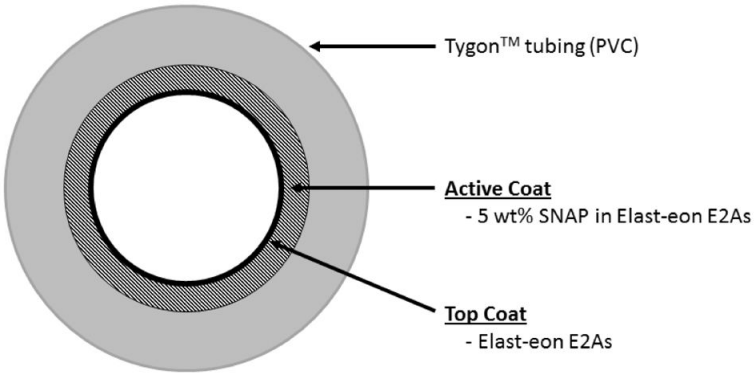

Fig. 7.
Diagram of the extracorporeal circuit (ECC) tubing coated with 5 wt% SNAP/E2As followed by a top coat of E2As.

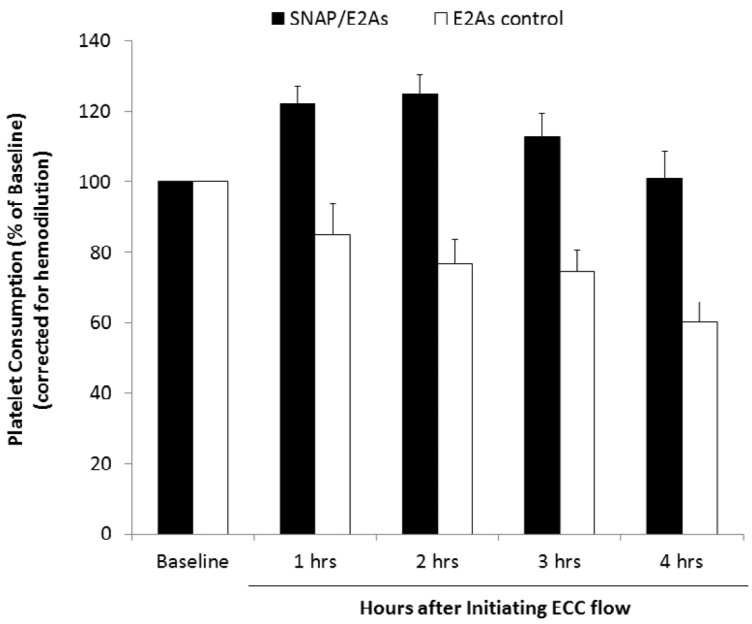

Fig. 8.

Time-dependent effects of the 5 wt% SNAP/E2As coating on platelet count (e.g. consumption) during the 4 h blood exposure in the rabbit thrombogenicity model. Data is the mean ± SEM (n=4).

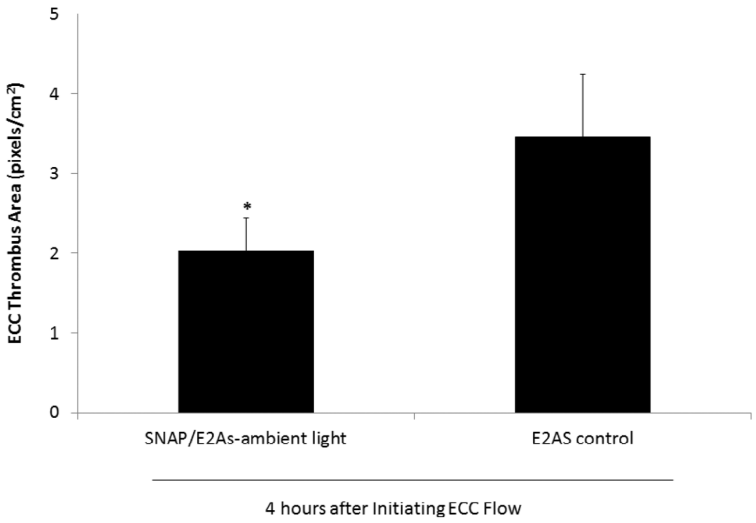

Fig. 9.

Two-dimensional representation of thrombus formation on the SNAP/E2As and control ECCs after 4 h blood exposure in the rabbit thrombogenicity model, as quantified using ImageJ software from NIH. Data is the mean ± SEM (n=4).